Lectures on effective field theory of large scale structure

Beta

Mehrdad Mirbabayi

Berlin, July 2018

Abstract: This is a preliminary version of a brief review of the EFT of LSS, the logic behind it and the way it works in practice. I will set up the perturbative expansion and discuss the examples of tree-level bispectrum, and 1-loop power spectrum where the counter-terms of the EFT that are needed to make sense of loops are introduced. I will then discuss infra-red resummation which explains broadening of the BAO peak. In the end, I will discuss the Zel'dovich approximation.

1 Introduction; the spherical collapse

Apart from understanding why the world around us is the way it is, an important motivation to study the dynamics of structure formation in the universe is to extract information about cosmological parameters such as σ_8, n_s, f_{NL}, m_ν, w, etc. Those parameters set the initial conditions and affect the dynamics and hence by a careful analysis what we observe can be translated into quantitative constraints.

The problem we are dealing with is the gravitational collapse of over-dense regions into halos, which when baryons are included, become hosts to galaxies we observe optically. Given that we are talking about collapsing objects, the nonlinearities are much more important compared to CMB. To warm up, let us study the collapse of a spherical over-density. In a matter dominated universe consider a spherical region of mass M, and comoving size R given by

$$M = \frac{4}{3}\pi R^3 \rho_0 \tag{1}$$

where ρ_0 is the comoving energy density. Take a Newtonian potential well of depth ϕ_0 within this region at initial times

$$\phi(\boldsymbol{x}) = \phi_0(1 - |\boldsymbol{x}|^2/R^2), \qquad |\boldsymbol{x}| < R, \tag{2}$$

and 0 outside, where $\boldsymbol{x}$ is the comoving coordinate. In linear perturbation theory, ϕ remains

constant in time, and implies a uniform density perturbations via Poisson equation

$$\frac{1}{a^2}\nabla^2\phi = 4\pi G\rho\delta \tag{3}$$

where I introduced the density contrast $\delta = \delta\rho/\bar{\rho}$, and $\bar{\rho}$ is the average density. For the above given ϕ we find at linear order (where ϕ remains constant) a uniform, growing density perturbation

$$\delta^{(1)} = -\frac{3\phi_0}{2\pi G\rho_0 R^2}a. \tag{4}$$

So the over-density is negligible at very early times. However, as time grows the region evolves as a closed cosmology which reaches a maximum radius and recollapses. This evolution can be solved for using Newtonian gravity. Tracking the trajectory of a particle at the boundary of the region, we have from energy conservation (here r is a physical length)

$$\dot{r}^2 = \frac{2GM}{r} + C, \qquad C < 0 \tag{5}$$

where C is related to ϕ_0. The solution is

$$r(\theta) = A(1 - \cos\theta), \qquad t(\theta) = B(\theta - \sin\theta) \tag{6}$$

with constants A, B given in terms of C by

$$A = -\frac{GM}{C}, \qquad B = \frac{A}{\sqrt{-C}}. \tag{7}$$

From (6) we see that the maximum radius is reached at $\theta = \pi$, and at

$$t_c = \pi B. \tag{8}$$

Hence, to determine the collapse time we need to find B. To do so note that at small times

$$\theta^2 = \theta_0^2 \left[1 + a_1\theta_0^2 + a_2\theta_0^4 + \mathcal{O}(\theta_0^6)\right], \qquad a_1 = \frac{1}{30}, \qquad a_2 = \frac{43}{25200},$$

$$\theta_0^2 \equiv \left(\frac{3!t}{B}\right)^{2/3} = \left(\frac{6}{B^2\pi G\rho_0}\right)^{1/3}a, \tag{9}$$

where I used the expression for the scale factor a in matter domination. (I keep the subsub-

leading terms for a later purpose.) Then r can be expanded as

$$r(t) = A(\frac{1}{2}\theta^2 - \frac{1}{4!}\theta^4 + \frac{1}{6!}\theta^6 + \cdots)$$

$$= \frac{A}{2}\theta_0^2 \left[(1 + a_1\theta_0^2 + a_2\theta_0^4) - \frac{2}{4!}\theta_0^2(1 + a_1\theta_0^2)^2 + \frac{2}{6!}\theta_0^4 + \mathcal{O}(\theta_0^6) \right] \tag{10}$$

$$= \frac{A}{2}\theta_0^2 \left[1 + b_1\theta_0^2 + b_2\theta_0^4 + \mathcal{O}(\theta_0^6) \right],$$

where

$$b_1 = a_1 - \frac{2}{4!} = -\frac{1}{20}, \qquad b_2 = a_2 - \frac{4a_1}{4!} + \frac{2}{6!} = -\frac{3}{2800}. \tag{11}$$

Then we solve for density

$$\rho(t) = \frac{3M}{4\pi r^3(t)} = \frac{6M}{\pi A^3 \theta_0^6} \left[1 + c_1\theta_0^2 + c_2\theta_0^4 + \mathcal{O}(\theta_0^6) \right], \tag{12}$$

where

$$c_1 = -3b_1 = \frac{3}{20}, \qquad c_2 = -3b_2 + 6b_1^2 = \frac{17}{21}c_1^2, \tag{13}$$

the second term in brackets in (12) gives $\delta^{(1)} = c_1\theta_0^2$. B can be solved for by comparing this to (4) and using (1), giving

$$t_c = \pi G M \left(\frac{c_1}{-\phi_0} \right)^{3/2}. \tag{14}$$

Given the initial statistics of ϕ perturbations, we can replace $-\phi$ by $\langle \phi(R)\phi(0) \rangle^{1/2}$ in this formula to estimate the time when typical halos of mass M collapse. Roughly, fluctuations with wave-number k correspond to collapsing regions of comoving size $1/k$.

1. *Calculate $\delta(t_c)$.*

2. *Show that the maximum radius of an over-density with the initial potential well ϕ_0 is*

$$HR_{\max} \sim \phi_0^{1/2}. \tag{15}$$

Our universe is not made just of matter, however many qualitative features of structure formation can be understood in a much easier way in matter-dominance. For this purpose one linearly evolves perturbations during the radiation epoch to obtain the initial condition for the subsequent period of matter dominance. Note that this evolution depends on the comoving momenta of the modes. The shorter wavelength modes $k > k_{\mathrm{eq}}$ which enter the horizon before matter-radiation equality (i.e. comoving scales for which $k/aH = 1$ before

3

equality time) suffer a suppression, while the longer wavelength modes remain conserved. The mapping between the primordial power spectrum, which is approximately scale invariant

$$\langle \zeta(\boldsymbol{k})\zeta(\boldsymbol{k}')\rangle = \frac{A}{k^{4-n_s}}(2\pi)^3\delta^3(\boldsymbol{k}+\boldsymbol{k}') \tag{16}$$

with $A \sim 10^{-10}$, and the spectrum of Newtonian potential ϕ at the beginning of the matter era is called the transfer function. At large scales $\phi_{k\ll k_{eq}} = -3\zeta/5$, while for $k > k_{eq}$ there is a suppression. It follows from (15) and smallness of ϕ that the structures form well inside the horizon.

The spherical collapse model is of course idealistic. The over-dense region collapses all the way until it forms a black hole. In reality, the collapsing regions are all embedded in one another and never perfectly spherical. As a result, after the collapse the constituent dark matter particles virialize. That is, the system stops collapsing when the kinetic energy K and potential energy U satisfy $K = -U/2$. We don't expect to be able to find an exact solution like the spherical collapse to the general problem, however we can use perturbation theory to go beyond the linear approximation. Given that structures collapse well inside the horizon, this allows us to access a larger range of modes by including those which are in the mildly nonlinear regime.

3. *Using the fact that at $r = r_{\max}$ the kinetic energy of the spherically collapsing region is zero, show that*

$$r_{\mathrm{vir}} = \frac{1}{2}r_{\max}. \tag{17}$$

2   Truncating Boltzmann Hierarchy; Cosmic Fluid

A collection of identical classical particles is in principle described by a distribution function $f(t,x,p)$ which gives the occupation of every cell in the phase space. Very often, at large enough distances an effective description arises. Hydrodynamics, elasticity, superfluidity are some examples. Suppose we apply the same logic and smooth the Boltzmann equation over some scale Λ. This is done in practice by integrating different quantities against a window function $W_\Lambda(\boldsymbol{x}-\boldsymbol{x}')$, e.g.

$$F_\Lambda(\boldsymbol{x}) = \int d\boldsymbol{x}' W_\Lambda(\boldsymbol{x}-\boldsymbol{x}')F(\boldsymbol{x}'), \qquad W_\Lambda(\boldsymbol{x}) = (\Lambda/\pi)^{3/2}e^{-\Lambda^2|\boldsymbol{x}|^2}. \tag{18}$$

One obtains (see sections 1.1 and 1.2 of http://physics.ipm.ac.ir/conferences/tmc/note/L.Senatore3.pdf)

$$\partial_\tau \delta + \partial_i[(1+\delta)v^i] = 0 ,$$

$$\partial_\tau v^i + \mathcal{H}v^i + \partial^i\phi + v^j\partial_j v^i = -\frac{1}{\rho}\partial_j \tau^{ij} \equiv -\frac{1}{(1+\delta)}\partial_j \tilde{\tau}^{ij} ,$$

(19)

where τ is the conformal time defined by $dt = a d\tau$ (τ^{ij} is a different thing, to be discussed at length below), $\mathcal{H} = \partial_\tau a/a$, $\Omega_m = 1$ in matter dominated universe. Density contrast δ and velocity v^i are defined in terms of the density field and momentum field

$$\rho = \bar{\rho}(1+\delta), \qquad v^i = \frac{\pi^i}{\rho}$$

(20)

and

$$\rho(t, \boldsymbol{x}) = \frac{m}{a^3}\int d^3\boldsymbol{p} f(t, \boldsymbol{x}, \boldsymbol{p}),$$

$$\pi^i(t, \boldsymbol{x}) = \frac{1}{a^4}\int d^3\boldsymbol{p} p^i f(t, \boldsymbol{x}, \boldsymbol{p}),$$

(21)

which are then filtered by W_Λ. I have dropped the subscript of ρ_Λ and π^i_Λ to avoid clutter. ϕ is related to δ via Poisson equation

$$\nabla^2\phi = \frac{3}{2}\mathcal{H}^2\Omega_m\delta .$$

(22)

The equations in (19) are just the expression of local conservation of mass and momentum. τ^{ij} on the r.h.s. of the momentum conservation is called the effective stress tensor and it is introduced such that if $\tau^{ij} = 0$ the equation reduces to the Euler equation for a pressureless fluid. τ^{ij} can be separated into kinetic and potential contributions

$$\tau^{ij} = \kappa^{ij} + \Phi^{ij}$$

(23)

where in particular

$$\kappa^{ij} = \sigma_\Lambda^{ij} - \rho v^i v^j$$

(24)

with

$$\sigma^{ij}(t, \boldsymbol{x}) = \frac{1}{ma^5}\int d^3\boldsymbol{p} p^i p^j f(t, \boldsymbol{x}, \boldsymbol{p}).$$

(25)

The expression for Φ^{ij} can be found in the above reference. Now one can ask if there is any sense in which τ^{ij} is small, and hence the matter fluctuations can be treated approximately

5

as a fluid. Generically, the answer is obviously negative, since we are dealing with very weakly interacting cold dark matter particles. We can have two streams moving in opposite directions through each other without much resistance. Then even though $\pi^i = \rho v^i$ could vanish, σ^{ij} and as a result τ^{ij} would be large. What allows fluid description to arise from a microscopic description of fluid constituents is the existence of a finite mean free path, given particle density n and cross section σ,

$$\ell = \frac{1}{n\sigma}, \tag{26}$$

so that over distances larger than ℓ, the motion of particles is fully correlated. There cannot be two streams at the same point if we take $\Lambda\ell \ll 1$.

Nonetheless, the fluid description is not totally hopeless, if we recall that our goal is to study structure formation. That is, the time-evolution of a very particular initial condition arising from adiabatic super-horizon perturbations. These are perturbations that start from vanishing initial velocity. As we saw in the spherical collapse problem the larger the mass (or equivalently, the smaller the wavenumber k) the longer it takes for the perturbations to collapse, which is approximately the time when multiple streams start appearing at those length scales. Hence, at any time t there is a range of long wavelength modes with $k < k_{\text{NL}}(t)$ for which the fluid description can be used [1004.2488].

There is another peculiar feature of the of the cosmic fluid. Even in the absence of any long wavelength perturbations, the system is violently out of equilibrium at short scales, since smaller halos keep forming and merging. Even though there is no correlation between far separated events, their random distribution contributes to momentum space correlation functions at small k. This is called Poisson noise or stochastic noise, and locality guarantees it to be analytic in momentum, as can be seen in the following example.

4. *Let's calculate the Poisson contribution to halo power-spectrum. Take a random distribution of halos with average density $\bar{n}_h$. To implement the randomness, divide the space into small cells of volume δv and introduce a random variable X_i for cell i which is 1 with probability $p = \bar{n}\delta v \ll 1$, and 0 otherwise. Define the halo density field as*

$$n_h(\boldsymbol{x}_i) = \frac{X_i}{\delta v}. \tag{27}$$

The Fourier transform of this is

$$n_h(\boldsymbol{k}) = \sum_i e^{i\boldsymbol{k}\cdot\boldsymbol{x}_i} X_i \tag{28}$$

Show that

$$\langle n_h(\boldsymbol{k})n_h(\boldsymbol{k}')' \rangle = \bar{n}_h (2\pi)^3 \delta^3(\boldsymbol{k} + \boldsymbol{k}'). \tag{29}$$

This is a k-independent power $P_h(k)$. Of course, at large enough k the halos can no longer be approximated as points and $P_h(k)$ starts to change. Experimentalists beautifully call this "shot noise".

However, there is no shot noise when discussing correlation functions of δ, the mass-density contrast. Peebles showed that energy and momentum conservation guarantees the stochastic contributions to $\delta(\boldsymbol{k})$ are $\mathcal{O}(k^2)$ rather than $\mathcal{O}(k^0)$ in the $k \to 0$ (see section 5 of 1509.07886). More importantly, given the source of the stochastic noise is collapsing structures of characteristic size $1/k_{\mathrm{NL}}$, this is an analytic expansion in k^2/k_{NL}^2 (this has to be the case since at $k \sim k_{\mathrm{NL}}$ we can no longer treat individual halos as point particles). Hence, for $k \ll k_{\mathrm{NL}}$ there is a well-defined perturbative expansion.

5. *τ^{ij} can have a uniform (zero-momentum) component. This is backreaction on the background FRW cosmology due to the perturbations. Show that for virialized objects this backreaction vanishes.*

3   Time-evolution, linear theory

To start I ignore τ^{ij} and solve the fluid equations to evolve the initial perturbations. First, we show that the source for vorticity $\omega^i = \epsilon^{ijk}\partial_j v_k$ vanishes in the absence of initial vorticity, and hence it remains zero given that it is zero initially. To see this, take the curl of the Euler equation and use

$$v^j \partial_j v^i = v^j(\epsilon^{jik}\omega_k + \partial_i v_j) = \epsilon^{jik} v_j \omega_k + \frac{1}{2}\partial_i(v^j v_j) \tag{30}$$

and use the fact that the curl of a gradient is zero, to obtain

$$\partial_\tau \omega^i + \mathcal{H}\omega^i + \partial_j(v^j \omega^i) - \partial_j(v^i \omega^j) = 0. \tag{31}$$

Vector perturbations decay outside of the horizon, so given that primordial fluctuations are super-horizon, the initial vorticity for our problem is zero, and it remains zero in Eulerian perturbation theory.

Hence, the velocity field can be written in terms of velocity divergence $\theta = \partial_i v^i$:

$$v^i = \frac{\partial_i}{\nabla^2}\theta. \tag{32}$$

So we need to solve for the coupled system of δ and θ. To set up the perturbative expansion, we first solve the linearized equations, derive the retarded Green's function, and treat nonlinearities as sources by evaluating them on the lower order solutions. At linear order

$$\theta^{(1)} = -\partial_\tau \delta^{(1)}, \tag{33}$$

taking the divergence of the Euler equation and using this relation we find

$$\partial_\tau^2 \delta^{(1)} + \mathcal{H} \partial_\tau \delta^{(1)} - \frac{3}{2} \mathcal{H}^2 \delta^{(1)} = 0, \tag{34}$$

or in terms of the scale factor

$$\mathcal{H}^2 [a^2 \partial_a^2 \delta^{(1)} + \frac{3}{2} a \partial_a \delta^{(1)} - \frac{3}{2} \delta^{(1)}] = 0. \tag{35}$$

The growing and decaying solutions are, respectively,

$$D_+ = a, \qquad D_- = a^{-3/2}. \tag{36}$$

Given the rapid decay of the decaying mode we will only keep the growing part of the solution. Hence, denoting the initial condition by $\delta_1(\boldsymbol{k})$ we have

$$\delta^{(1)}(\boldsymbol{k}) = a \delta_1(\boldsymbol{k}) \tag{37}$$

so the linear power spectrum grows as a^2

$$\left\langle \delta^{(1)}(\boldsymbol{k}) \delta^{(1)}(\boldsymbol{k}') \right\rangle = a^2 P_{11}(k)(2\pi)^3 \delta^3(\boldsymbol{k} + \boldsymbol{k}'). \tag{38}$$

As expected, linear perturbations grow in time, and thus nonlinearities eventually become non-negligible. If we ask what is the typical amplitude of perturbations with comoving size R at time t, it could be determined from

$$\langle \delta(t, \boldsymbol{x}) \delta(t, 0) \rangle = \int \frac{d^3 \boldsymbol{k}}{(2\pi)^3} P(k, t) e^{i\boldsymbol{k} \cdot \boldsymbol{x}}, \qquad |\boldsymbol{x}| = R. \tag{39}$$

The linear theory predicts that this becomes $\mathcal{O}(1)$ when

$$\Delta(k) = a^2 k^3 P_{11}(k) = 1 \tag{40}$$

for $k \sim 1/R$. As we will see $\Delta(k)$ is the loop expansion parameter.

Next, we find the retarded Green's function, which is the solution to

$$\mathcal{H}^2[a^2\partial_a^2 G(a,a') + \frac{3}{2}a\partial_a G(a,a') - \frac{3}{2}G(a,a')] = \delta(a-a'), \tag{41}$$

with the condition that $G(a < a', a') = 0$. The solution is

$$G(a > a', a') = \frac{2}{5H_0}\left[\frac{a}{a'} - \left(\frac{a'}{a}\right)^{3/2}\right], \tag{42}$$

where I used $\mathcal{H} = H_0/a^{1/2}$ in matter dominated universe.

# 4 Second-order solution and tree-level bispectrum

Our next goal is to include nonlinearities. It is very useful to have a diagrammatic representation to organize various terms in perturbation theory. In our problem, these are time-evolution diagrams which tell us how n initial fields evolve into a final $\delta^{(n)}$. Graphically, they are all trees (or rather roots). When working with density and velocity field the nonlinearities are two quadratic terms from continuity and Euler equations, respectively,

$$\alpha = -\partial_i(\delta v^i), \tag{43}$$

and

$$\beta = -\partial_i(v^j\partial_j v^i). \tag{44}$$

So the diagrams only have cubic vertices which combine two incoming field into one outgoing. For instance, one diagram contributing to the forth order solution $\delta^{(4)}$ is

$$\tag{45}$$
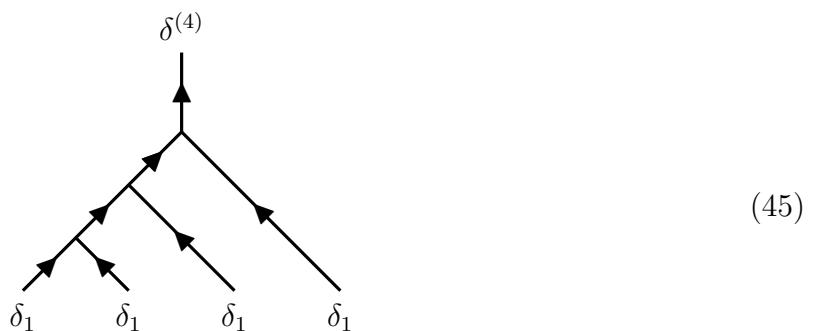
See 1509.07886 for more examples and diagrammatic rules.

The nonlinear equation for δ is

$$\mathcal{H}^2[a^2\partial_a^2\delta + \frac{3}{2}a\partial_a\delta - \frac{3}{2}\delta] = -\beta + \mathcal{H}(a\partial_a + 1)\alpha, \tag{46}$$

which is solved for $\delta^{(n)}$ by substituting the lower order solutions $\delta^{(m<n)}, \theta^{(m<n)}$ in the r.h.s. and using the $G(a, a')$. Given the solutions $\delta^{(m\le n)}$ and $\theta^{(m<n)}$ one can use $\theta = -\partial_\tau\delta + \alpha$ to solve for $\theta^{(n)}$ and proceed to the next order.[1]

At second order, the source term for δ is (suppressing the $\boldsymbol{x}$ argument)

$$S_\delta(a) = H_0 a \left[\frac{5}{2}\partial_i\left(\delta_1\frac{\partial_i}{\nabla^2}\delta_1\right) + \partial_i\left(\frac{\partial_i}{\nabla^2}\delta_1\frac{\partial_i\partial_j}{\nabla^2}\delta_1\right)\right]. \tag{47}$$

Integrating this against $G(a, a')$, gives

$$\delta^{(2)}(a) = \int^a da' G(a, a')S_\delta(a') = \frac{2a}{7H_0}S_\delta(a). \tag{48}$$

Simplifying the result gives

$$\delta^{(2)} = a^2\left[\frac{5}{7}\delta_1^2 + \frac{2}{7}\left(\frac{\partial_i\partial_j}{\nabla^2}\delta_1\right)^2 + \frac{\partial_i}{\nabla^2}\delta_1\partial_i\delta_1\right]. \tag{49}$$

6. *Find $\theta^{(2)}$.*

7. *Most of the times we are interested in expression in momentum space. So we write $\delta^{(2)} = a^2\delta_2$ with*

$$\delta_2(\boldsymbol{k}) = \int \frac{d^3\boldsymbol{q}_1}{(2\pi)^3}\frac{d^3\boldsymbol{q}_2}{(2\pi)^3}F_2(\boldsymbol{q}_1, \boldsymbol{q}_2)\delta_1(\boldsymbol{q}_1)\delta_1(\boldsymbol{q}_2)(2\pi)^3\delta^3(\boldsymbol{q}_1 + \boldsymbol{q}_2). \tag{50}$$

(Below I'll keep the momentum conserving delta function and the measure $d^3\boldsymbol{q}_i$ implicit.) Find F_2.

In cosmology we have at best a probabilistic description of the initial condition, so we can only make predictions about correlation functions. Those who are interested in inflation have certainly heard about primordial non-Gaussianities and 3-point correlation function, or bispectrum. Given $\delta^{(2)}$ we are now able to find the leading non-primordial contribution to

---

[1]We could also try to solve for v^i in terms of δ and obtain an equation for a single variable. However, this doesn't seem to be a very smart choice, since instead of only two cubic vertices, the resulting theory would have vertices at all orders.

the bispectrum (called B_{211}):

$$\langle \delta(\boldsymbol{k}_1)\delta(\boldsymbol{k}_2)\delta(\boldsymbol{k}_3)\rangle = a^4 \langle \delta_2(\boldsymbol{k}_1)\delta_1(\boldsymbol{k}_2)\delta_1(\boldsymbol{k}_3)\rangle + \text{permutations}$$

$$= a^4[F_2(\boldsymbol{k}_2, \boldsymbol{k}_3)P_{11}(k_2)P_{11}(k_3) + \text{perms.}](2\pi)^3\delta^3(\boldsymbol{k}_1 + \boldsymbol{k}_2 + \boldsymbol{k}_3). \tag{51}$$

Let us compare the size of this to primordial non-Gaussianities, which can be understood as having a Newtonian potential which is nonlinearly related to a Gaussian variable

$$\phi = g + f_{\mathrm{NL}}g^2, \tag{52}$$

with $f_{\mathrm{NL}} \sim 1$ being an interesting target after Planck. This leads to a bispectrum for δ, which for $k_1 \sim k_2 \sim k_3$ is

$$\langle \delta(\boldsymbol{k}_1)\delta(\boldsymbol{k}_2)\delta(\boldsymbol{k}_3)\rangle'_{\mathrm{primordial}} \sim \frac{f_{\mathrm{NL}}\mathcal{H}^2}{k_1^2 T(k_1)}P_{11}^2(k_1) \tag{53}$$

where prime denotes stripping off the momentum conserving delta function, and $T(k)$ is the transfer function: $T(0) = 1$ and $T(k > k_{\mathrm{eq}}) \sim k_{\mathrm{eq}}^2/k^2$. On the same equilateral configuration $F_2 \sim 1$, and hence

$$\frac{B_{\mathrm{primordial}}}{B_{211}} \sim \frac{f_{\mathrm{NL}}\mathcal{H}^2}{k^2 T(k)} \ll 1, \tag{54}$$

for most of the observable modes. For instance, at $k = 0.03h/\mathrm{Mpc}$ this ratio is $\mathcal{O}(10^{-3})$. Thus for many purposes, we need to understand structure formation at nonlinear level to be able to use LSS data. Indeed, as long as the perturbation parameter $\Delta(k) > 10^{-3}$, we have to proceed to subleading orders in perturbation series to reach the desired precision. That is, we need to calculate loops.[2]

8. *Use induction to show that the perturbation theory solution for δ and θ is of the form*

$$\delta(t, \boldsymbol{x}) = \sum_{n=1}^{\infty} a^n \delta_n(\boldsymbol{x}), \qquad \theta(t, \boldsymbol{x}) = \mathcal{H}\sum_{n=1}^{\infty} \theta_n(\boldsymbol{x}). \tag{55}$$

Show that δ_n and θ_n satisfy the following recursive relations

$$\delta_n = \frac{1}{(n-1)(n+3/2)} \sum_{\substack{m_1+m_2=n \\ m_1>0, m_2>0}} \partial_i(v_{m_1}^j \partial_j v_{m_2}^i) - (n+1/2)\partial_i(\delta_{m_1}v_{m_2}^i). \tag{56}$$

Transform this to momentum space and find the recursive relations in eqs. 43, 44 of

[2]Some estimates of this sort for various cosmological parameters and their prospects from the near future LSS observations can be found in 1602.00674.

0112551.

9. *Reproduce the second order terms in the spherical collapse solution by taking angular average of $\delta^{(2)}$.*

10. *Show that in the "squeezed limit", $k_1 \ll k_2$,*

$$F_2(\boldsymbol{k}_1, \boldsymbol{k}_2) \simeq \frac{\boldsymbol{k}_1 \cdot \boldsymbol{k}_2}{2k_1^2} \gg 1, \tag{57}$$

while B_{211} has no $1/k_1$ divergence. What about the unequal time 3-point function? These relations are tree-level examples of what is called LSS consistency relations 1311.0290. In the vicinity of the BAO feature the equal-time consistency relation becomes nontrivial 1504.04366.

Finally, we can also have a diagrammatic representation for various terms in the correlation functions. We need an extra ingredient, which is the initial correlation of δ_1 fields. When two initial fields are correlated we represent it by a dot. Time flows away from the dots and towards the external legs. An example of a diagram contributing to the 6-point correlation function is

$$\tag{58}$$
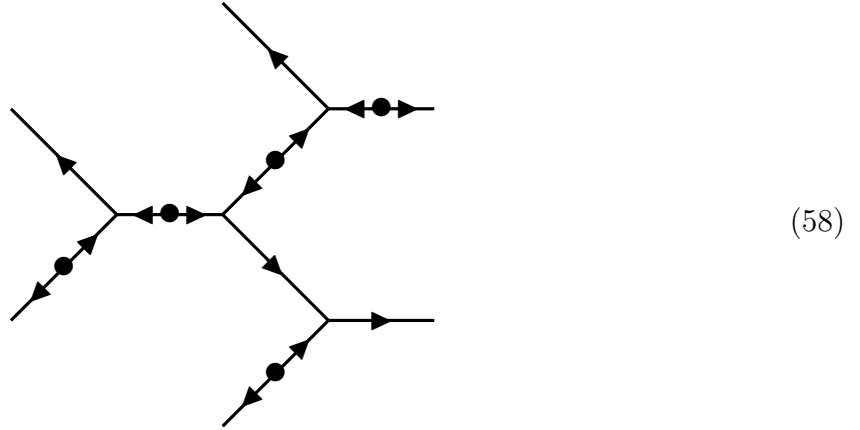
This is called a tree diagram, because all internal momenta are determined by the external ones. They give the leading contribution to the correlation functions. Once we go to higher order in Δ contributions, we have loop diagrams.

11. *Draw the diagrams for B_{211}.*

5   Loops and counter-terms

So far we learned that in the mildly nonlinear regime one can expand density and velocity fields as a power-series in the initial perturbations:

$$\delta_n(\boldsymbol{k}) = \frac{1}{n!} \int_{\sum \boldsymbol{q}_i = \boldsymbol{k}} F_n(\boldsymbol{q}_1, \cdots, \boldsymbol{q}_n) \delta_1(\boldsymbol{q}_1) \cdots \delta_1(\boldsymbol{q}_n). \tag{59}$$

However, the indefinite momentum integrals inevitably introduce error in our result, since at any moment, there is a finite range of modes with $k \ll k_{\mathrm{NL}}$ which are described by the fluid equations. At tree-level, this is not an issue because all momenta are fixed by the external ones, which can be taken to be soft. However, at subleading order some of the integrals survive and have to be dealt with in a proper way. I'll demonstrate this in the example of 1-loop power spectrum.
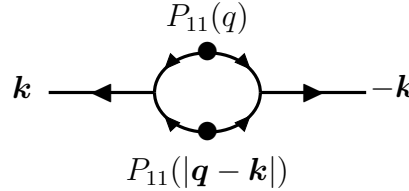
To next-to-leading order

$$\langle \delta(t, \boldsymbol{k}) \delta(t, -\boldsymbol{k}) \rangle' = \langle \delta^{(1)}(\boldsymbol{k}) \delta^{(1)}(-\boldsymbol{k}) \rangle' + \langle \delta^{(2)}(\boldsymbol{k}) \delta^{(2)}(-\boldsymbol{k}) \rangle' + 2 \langle \delta^{(1)}(\boldsymbol{k}) \delta^{(3)}(-\boldsymbol{k}) \rangle' = a^2 P_{11} + a^4 P_{22} + a^4 P_{13} \tag{60}$$

where

$$P_{22}(k) = 2 \int_{\boldsymbol{q}} F_2^2(\boldsymbol{q}, -\boldsymbol{q} + \boldsymbol{k}) P_{11}(q) P_{11}(|\boldsymbol{q} - \boldsymbol{k}|), \tag{61}$$

is diagrammatically represented by
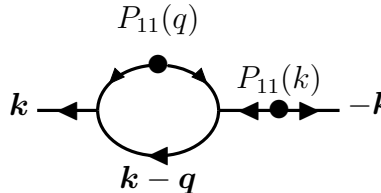
$$\tag{62}$$

and

$$P_{13}(k) = 6 P_{11}(k) \int_{\boldsymbol{q}} F_3(\boldsymbol{q}, -\boldsymbol{q}, \boldsymbol{k}) P_{11}(q). \tag{63}$$

by

$$\tag{64}$$

As anticipated there is contribution from all momenta, including those beyond k_{NL}. To fix this we could cutoff the integrals at some momentum $\Lambda \gg k$, however the result would then

depend on our arbitrary choice of the cutoff. Moreover, for any reasonable choice of Λ near k_{NL}, we make some error by excluding the contribution of short modes above Λ, and by inaccurate evaluation of the effect of those below Λ. The role of the effective stress tensor, which we neglected so far, is to fix both of these problems. Generically, the its structure (i.e. momentum dependence) can be determined by investigating the cutoff dependence of the loop. Thus we need to understand various limits of the perturbation theory kernels F_n.

5.1 Perturbation theory kernels

The first property of the F_n kernels is their overall scale invariance:

$$F_n(\lambda \boldsymbol{k}_1, \cdots, \lambda \boldsymbol{k}_n) = F_n(\boldsymbol{k}_1, \cdots, \boldsymbol{k}_n). \tag{65}$$

The second property is IR safety: Consider a time-evolution diagram which includes some high momentum (hard) modes and some soft modes. As we saw in the example of F_2 kernel, the leading coupling of the two modes $\boldsymbol{k}$ and $\boldsymbol{q}$ with $k \ll q$ is

$$\frac{\boldsymbol{k} \cdot \boldsymbol{q}}{k^2} = \mathcal{O}(q/k). \tag{66}$$

This is called an infrared ($k \to 0$) singularity. This comes from the $v^i \partial_i \delta$ and $v^i \partial_i \theta$ terms in the evolution equations and it is dictated by the Equivalence Principle. A long wavelength mode $\delta(\boldsymbol{q}_1)$ sources a gravitational field in which all smaller scale structures fall together. Hence, the coefficient of this coupling is universally 1. It follows that if several hard momenta add up to a soft momentum in a time-evolution diagram, the IR divergence due to attachment of a soft velocity field cancels instantaneously. To see this freeze the rest of diagram and at any given time t_0 sum over all attachments of the soft velocity to get

$$\theta(t_0, \boldsymbol{k}) \sum_i \frac{\boldsymbol{k} \cdot \boldsymbol{q}_i}{k^2} A(\boldsymbol{q}_1, \cdots, \boldsymbol{q}_i + \boldsymbol{k}, \cdots) \tag{67}$$

where A is the amplitude for the rest of the diagram. In the $k \ll q$ limit we can neglect the change in the argument of A and obtain

$$\theta(t_0, \boldsymbol{k}) A(\boldsymbol{q}_1, \cdots) \sum_i \frac{\boldsymbol{k} \cdot \boldsymbol{q}_i}{k^2} = \theta(t_0, \boldsymbol{k}) A(\boldsymbol{q}_1, \cdots) \frac{\boldsymbol{k} \cdot \boldsymbol{q}_{\mathrm{tot}}}{k^2} + \mathcal{O}(k^0). \tag{68}$$

Hence, if the total momentum in the diagram is small the soft velocity does not lead to any IR growth.

The third property of F_n kernels is their double-softness when two almost equal but

14

opposite hard momenta $\mathcal{O}(q)$ combine to give a soft mode $\mathcal{O}(k)$. This can be seen by a rewriting (following Goroff-Grinstein-Rey-Wise) of the source term S_δ in the evolution equation (46):

$$S_\delta = \partial_i\partial_j(v^i\pi^j) + \frac{2}{3\mathcal{H}^2}[\partial_i\partial_j(\partial_i\phi\partial_j\phi) - \frac{1}{2}\nabla^2(\partial_k\phi\partial_k\phi)]. \tag{69}$$

One subtlety (discussed in 1509.07886) is that for the double softness of the whole diagram to follow, one needs to insure there is no IR divergence in the diagram, as we did. Combined with the first property (65), we conclude that

$$\lim_{\lambda\to\infty} F_n(k_1,\cdots,k_{n-2},\lambda\boldsymbol{k}_{n-1},\lambda\boldsymbol{k}_n) = \mathcal{O}(1/\lambda^2). \tag{70}$$

12. *Derive* (69)

5.2 Counter-terms

Let's return to P_{22} and P_{13} diagrams and renormalize them. For this we need to look at the UV limit of the loop momentum $q \gg k$. Then P_{22} diagram correlates two $\delta^{(2)}(k)$ which are formed from two hard modes of momentum $\boldsymbol{q}$ and $\boldsymbol{k}-\boldsymbol{q}$. From the above discussion we know that each of these comes with a k^2 factor, and hence

$$P_{22}^{\text{UV}} \propto k^4. \tag{71}$$

In the P_{13} diagram we have one $\delta^{(3)}(k)$ which is formed by combining two short mode and a $\delta_1(\boldsymbol{k})$, so we have

$$P_{13}^{\text{UV}} \propto k^2 P_{11}(k). \tag{72}$$

To renormalize 1-loop power spectrum, we just need to add two counter-terms whose k-dependence match the UV behavior of these two diagrams. The first one, is a stochastic counter-term. As we discussed the UV limit of P_{22} diagram corresponds to the possibility that even in the absence of initial long wavelength perturbations, they will form via the evolution and collapse of the shorter scales. This stochastic noise is analytic in momentum (corresponding to local, uncorrelated processes in real space), and as promised for mass density contrast δ, it starts from k^2.

The counter-term corresponding to P_{13}, on the other hand, depends on an initially existing long mode. It corresponds to the fact that the evolution of short wavelength perturbations is modified in the presence of the long mode. This modification must be through locally observable effect, such as the change in the local expansion rate $\propto \delta_1(\boldsymbol{k})$, or the tidal shear $\partial_i\partial_j\phi$. Hence, the effective stress tensor τ^{ij} would depend on these. To obtain the

source for δ one acts by two more derivatives (see (19) and recall that we take divergence of the Euler equation to obtain evolution equation for δ). Hence, at this order we have

$$\delta_{\text{ct}}(\boldsymbol{k}) = \ell_{22}^2(t)k^2 J(\boldsymbol{k}) + \ell_{13}^2(t)k^2 a\delta_1(\boldsymbol{k}), \tag{73}$$

where J is a delta-function correlated random variable $\langle J(\boldsymbol{k})J(\boldsymbol{k}')\rangle = (2\pi)^3\delta^3(\boldsymbol{k}+\boldsymbol{k}')$. The renormalized 1-loop power spectrum is

$$P_{1-\text{loop}}(k) = a^4 P_{22} + a^4 P_{13} + 2\ell_{13}^2(t)k^2 a^2 P_{11}(k) + \ell_{22}^4(t)k^4. \tag{74}$$

This 1-loop result has two parameters $\ell_{13}(t)$ and $\ell_{22}(2)$ which will depend on the regularization scheme (e.g. on Λ, if we cutoff the loops). If the loops are cutoff at $\Lambda \sim k_{\text{NL}}$, then one would expect both $\ell_{13}, \ell_{22} \sim 1/k_{\text{NL}}$. They characterize our ignorance about the short scale dynamics. Note however that the collapse of cold dark matter is a well-defined problem which can in principle be solved numerically to obtain the values of these coefficients.[3]

Finally, I should mention that depending on the initial power spectrum different 1-loop counter-terms would be of different degree of importance. To understand this it is useful to estimate the 1-loop result by dividing it into the contribution from the loop momenta $q \sim k$, plus the UV part which is degenerate with the counter-terms:

$$P_{1-\text{loop}}(k) \sim a^2 P_{11}(\Delta(k) + (k/k_{\text{NL}})^2) + \frac{k^4}{k_{\text{NL}}^7}. \tag{75}$$

In our universe the power spectrum in the mildly nonlinear scale can be approximated by a power-law k^n with $n \simeq -1.5$. This gives $\Delta \sim (k/k_{\text{NL}})^{3+n} \sim (k/k_{\text{NL}})^{1.5}$. Hence, the UV contributions become less important at smaller k. At l loops the $q \sim k$ contribution of loop diagrams would go as Δ^l, so in our universe the ℓ_{13} counter-term is more relevant than 2-loop diagrams.

It can be seen in Fig. 1 that adding ℓ_{13} counter-term significantly improves the reach of perturbations theory (i.e. it increases the maximum k that the theory fits simulations within say 1% error). This a framework that allows systematic improvement at $k \ll k_{\text{NL}}$. The structure of counter-terms as we go to higher orders become more complicated, but we have finally understood how to systematically construct and count them to all orders [see for instance 1509.07886, 1511.01889].

However, this improvement comes at the expense of having more and more free parameters analogous to ℓ_{13}. As a result with a finite data set, the improvement saturates. This is not unexpected, effective field theories are great in determining the universal features of IR

---

[3]One-loop power spectrum was first studied in the context of EFT in 1206.2926.
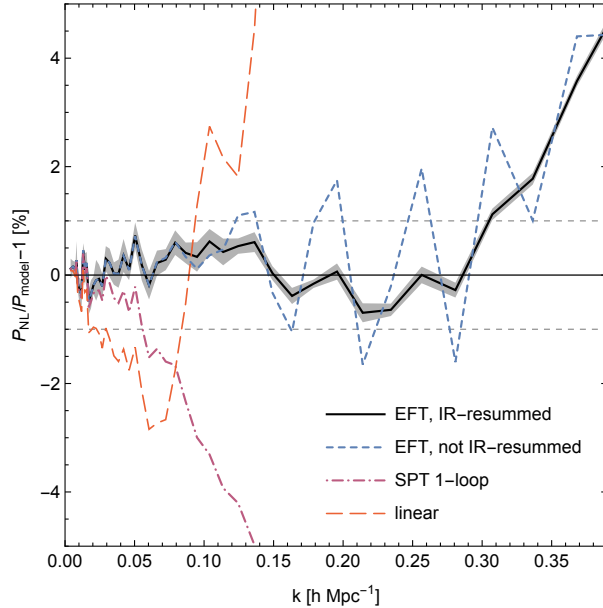
Figure 1: *The ratio of various theoretical approximations to the power spectrum to the simulation result. Solid: IR-resummed, short-dashed: 1-parameter 1-loop EFT, dot-dashed: 0-parameter 1-loop EFT with $R = 0$, and long-dashed: linear. The gray shaded region on the IR-resummed EFT curve gives the statistical error.*

physics, but they are not tools for marching towards UV.

6   BAO and IR-resummation

As seen in Fig. 1, the 1-loop EFT power spectrum has large oscillations with respect to the simulation results. The source of these oscillation is BAO, and it is understood how to deal with them in perturbation theory. The physics behind this mismatch can be best understood by thinking about the real-space correlation function. This correlation function has a peak at the scale $\ell_{\rm BAO} \sim 100 h^{-1} {\rm Mpc}$. It can be thought of as preferential clustering at a distance $\ell_{\rm BAO}$ from any over-density. However, the motion v^i due to modes with wavelength between that scale and the width of the peak $\sigma \ll \ell_{\rm BAO}$ significantly distorts the shape of the (hypothetical) BAO shell that surrounds every over-dense region, leading to a broader peak. In fact, this broadening can be calculated equally well for any biased tracer, since by the Equivalence Principle everything falls in the same way in a long wavelength gravitational fields, with deviations suppressed by additional derivatives.[4]

---

[4]What follows is based on 1504.04366. For a pioneering work on BAO broadening and reconstruction see 0604362. In the context of EFT, IR-resummation was first discussed in 1404.5954.

6.1 Squeezed Bispectrum

Consider a long wavelength mode $\delta_L(\tau, \boldsymbol{x}) = \delta_{\boldsymbol{q}}(\tau) \cos(\boldsymbol{q} \cdot \boldsymbol{x})$. By the above argument the motion in the gravitational field of this mode is easiest to find from matter equations of motion. For matter, the linearized continuity equation implies $\boldsymbol{v} \simeq -\frac{\nabla}{\nabla^2} \partial_\tau \delta$. The total displacement since $\tau = 0$ is then

$$\Delta \boldsymbol{x} = -\delta_{\boldsymbol{q}}(\tau) \sin(\boldsymbol{q} \cdot \boldsymbol{x}) \, \boldsymbol{q}/q^2. \tag{76}$$

13. *Derive this equation.*

Cosmological observables (like galaxies) are often observed at a single point in their lifespan. Hence, even though $\Delta \boldsymbol{x}$ depends on $\boldsymbol{x}$, the relative motion of any given pair of points is impossible to determine, since we don't know where they have started from. What is possible is to see how the distribution of pairs is correlated with δ_L. For pairs of any objects, say galaxies, equation (76) implies

$$\left\langle \delta_g(\frac{\boldsymbol{x}}{2}, \tau) \delta_g(-\frac{\boldsymbol{x}}{2}, \tau) \right\rangle_{\delta_L} \simeq \xi_g(\boldsymbol{x}, \tau) + 2\delta_{\boldsymbol{q}}(\tau) \sin\left(\frac{\boldsymbol{q} \cdot \boldsymbol{x}}{2}\right) \frac{\boldsymbol{q}}{q^2} \cdot \nabla \xi_g(\boldsymbol{x}, \tau), \tag{77}$$

where $\xi_g(\boldsymbol{x}, t)$ is an average 2-point correlation function, of galaxy density contrast. Not surprisingly, the distribution of pairs with separation much less than the long wavelength, $\boldsymbol{q} \cdot \boldsymbol{x} \ll 1$, is hardly affected by the long mode. The second line would in this case correspond to the effect of living in an over (under) dense Universe. An effect of order $\delta_L x |\nabla \xi_g|$, which for an approximately scale invariant spectrum, $|\nabla \xi_g(\boldsymbol{x}, t)| \sim \xi_g(\boldsymbol{x}, t)/x$, is comparable to dynamical contributions of order $\delta_L \xi_g$, which are neglected anyway on the right-hand side. By dynamical contribution I mean the modification of the correlation function because in the presence of the long mode the short wavelength modes experience a different background cosmology (e.g. recall that an over-dense spherical region is like a closed cosmology).

However, even if $\boldsymbol{q} \cdot \boldsymbol{x} \gg 1$, when we do expect the long-wavelength mode to induce a large relative motion, the second line of (77) is often negligibly small. Scale invariance now implies that it is of order $\delta_L \xi_g/qx$.

The relative motion is noticeable only if the distribution of pairs has a feature such that the derivative of ξ on the r.h.s. of (77) becomes large. One such feature does exist in the Universe at the baryon acoustic oscillation peak. For $x \sim \ell_{\text{BAO}}$,

$$|\nabla \xi_g| \sim \frac{1}{\sigma} \xi_g \gg \frac{1}{\ell_{\text{BAO}}} \xi_g, \tag{78}$$

where σ is the width of the peak. At this separation, the effect of the long mode on the

distribution of pairs is of order $\delta_L \ell_{\mathrm{BAO}} \xi_g / \sigma$ for $q \ll \ell_{\mathrm{BAO}}^{-1}$, and $\delta_L \xi_g / q\sigma$ for $\ell_{\mathrm{BAO}}^{-1} \ll q \ll \sigma^{-1}$, which are both dominant compared to the $\mathcal{O}(\delta_L \xi_g)$ dynamical effects.

An approximate three-point correlation function can be obtained in this regime by correlating (77) with $\delta(\boldsymbol{q}, \tau)$ to get

$$\left\langle \delta(\boldsymbol{q}, \tau) \delta_g(\frac{\boldsymbol{x}}{2}, \tau) \delta_g(-\frac{\boldsymbol{x}}{2}, \tau) \right\rangle \simeq 2 P_{\mathrm{lin}}(q, \tau) \sin\left(\frac{\boldsymbol{q} \cdot \boldsymbol{x}}{2}\right) \frac{\boldsymbol{q}}{q^2} \cdot \nabla \xi_g(\boldsymbol{x}, \tau), \tag{79}$$

where $P_{\mathrm{lin}}(q, t)$ is the linear matter power spectrum $(= a^2 P_{11}(q)$ during matter domination).

6.2 Large-scale displacements at one loop

Intuitively, the above result describes how galaxy pairs, which are more likely to be found at distance ℓ_{BAO}, are moved to larger or smaller separations in the presence of a mode of wavelength longer than σ. When averaged over the long modes, these motions lead to the well-known spread of the acoustic peak.

For this purpose, it is necessary to keep higher order terms in the expansion (77). At second order in relative displacement, now caused by the modes $\boldsymbol{q}_1$ and $\boldsymbol{q}_2$, the r.h.s. reads

$$2 \delta_{\boldsymbol{q}_1}(\tau) \delta_{\boldsymbol{q}_2}(\tau) \sin\left(\frac{\boldsymbol{q}_1 \cdot \boldsymbol{x}}{2}\right) \sin\left(\frac{\boldsymbol{q}_2 \cdot \boldsymbol{x}}{2}\right) \frac{q_1^i q_2^j}{q_1^2 q_2^2} \partial_i \partial_j \xi_g(\boldsymbol{x}, \tau). \tag{80}$$

As before, this is the leading effect of the long mode if $x \approx \ell_{\mathrm{BAO}}$, and ξ_g is the correlation function in the absence of the q modes. By correlating (80) with two long modes one can obtain the double-squeezed four-point correlation function. Alternatively, averaging over the long modes with $q < \lambda \ll 2\pi\sigma^{-1}$, gives the first correction to the observed two-point correlation around the peak:

$$\tilde{\xi}_g(r, \tau) \approx \xi_{g,L}(r, \tau) + \xi_{g,S}(r, \tau) + \Sigma_\lambda^2 \xi_{g,S}''(r, \tau), \tag{81}$$

where $r \equiv |\boldsymbol{x}|$, prime denotes $\partial/\partial r$, and terms suppressed by $\sigma/\ell_{\mathrm{BAO}}$ are neglected. $\xi_{g,L}(\boldsymbol{x}, \tau)$ – the direct contribution of the long-modes to the correlation function – and $\xi_{g,S}(\boldsymbol{x}, \tau)$ – that of the short modes in the absence of the long modes– are assumed to be isotropic. Note that while $\xi_{g,S}$ contains the full short scale nonlinearities, only the leading effect of the long modes on the short modes has been kept in (81). For each q mode, this scales as $P_{\mathrm{lin}}(q)(\ell_{\mathrm{BAO}}/\sigma)^2$ for $q \ll \ell_{\mathrm{BAO}}^{-1}$, and $P_{\mathrm{lin}}(q)/(q\sigma)^2$ for $q > \ell_{\mathrm{BAO}}$. The neglected terms are suppressed by one or more powers of $\sigma/\ell_{\mathrm{BAO}}$ and $q\sigma$, respectively. Hence, due to the bulk motions, $\tilde{\xi}_g$ has a

broader peak with Σ_λ^2 given by

$$\Sigma_\lambda^2 \approx \frac{1}{6\pi^2} \int_0^\lambda \mathrm{d}q \, P_{\mathrm{lin}}(q)[1 - j_0(q\ell_{\mathrm{BAO}}) + 2j_2(q\ell_{\mathrm{BAO}})], \tag{82}$$

where j_n is the nth order spherical Bessel function.

14. *One can perturbatively confirm the above result when ξ_g is taken to be the matter correlation: Show that the leading contribution of the long wavelength modes $q \ll k$ to the one-loop power spectrum (i.e. P_{22} and P_{13} diagrams) is*

$$P_{1-\mathrm{loop}}^w(k > \lambda) = \frac{1}{2} \int^\lambda \frac{\mathrm{d}^3\boldsymbol{q}}{(2\pi)^3} \frac{(\boldsymbol{q} \cdot \boldsymbol{k})^2}{q^4} P_{\mathrm{lin}}(q)[P_{\mathrm{lin}}(|\boldsymbol{k}+\boldsymbol{q}|)+P_{\mathrm{lin}}(|\boldsymbol{k}-\boldsymbol{q}|)-2P_{\mathrm{lin}}(k)] \ . \tag{83}$$

Next separate P_{lin} into an oscillating piece P^w and a smooth piece P^{nw}:

$$P_{\mathrm{lin}}(k) = P_{\mathrm{lin}}^w + P_{\mathrm{lin}}^{nw}(k) \tag{84}$$

where $P_{\mathrm{lin}}^w \propto \sin(\ell_{\mathrm{BAO}}k)$ times a smooth envelope. Show that for $q \ll k$ the expression in the square brackets simplifies to $-4P_{\mathrm{lin}}^w(k)\sin^2(\boldsymbol{q} \cdot \hat{\boldsymbol{k}}\ell_{\mathrm{BAO}}/2)$, up to terms which are suppressed by q/k. Hence, giving

$$P_{1-\mathrm{loop}}^w(k > \lambda) = \Sigma_\lambda^2 k^2 P_{\mathrm{lin}}^w(k), \tag{85}$$

and taking the Fourier transform with respect to $\boldsymbol{k}$ reproduces (81).

However, the 1-loop result gives a very bad prediction for the nonlinear real-space correlation function at ℓ_{BAO}. This is because the variance of displacements Σ is too big to be treated perturbatively. In the momentum space, this failure is apparent from large oscillations of the 1-loop EFT result for $P(k)$ in fig. 1.

6.3 Infra-red resummation and BAO broadening

We can obtain a better formula which is valid to all orders in the relative displacement $\delta_{\boldsymbol{q}}/q$, by rewriting (77) as

$$\left\langle \delta_g(\frac{\boldsymbol{x}}{2}, t)\delta_g(-\frac{\boldsymbol{x}}{2}, t) \right\rangle_{\delta_L} \simeq \int \frac{\mathrm{d}^3\boldsymbol{k}}{(2\pi)^3} \, e^{i\boldsymbol{k}\cdot\boldsymbol{x}} \exp\left[2i\delta_{\boldsymbol{q}}(\tau)\sin\left(\frac{\boldsymbol{q}\cdot\boldsymbol{x}}{2}\right)\frac{\boldsymbol{q}\cdot\boldsymbol{k}}{q^2}\right] \langle \delta_g(\boldsymbol{k}, t)\delta_g(-\boldsymbol{k}, t) \rangle \ . \tag{86}$$

As before, this is only relevant in the presence of a feature. Taking the expectation value over the realizations of the q modes, approximating them, as we did so far, as being Gaussian, and
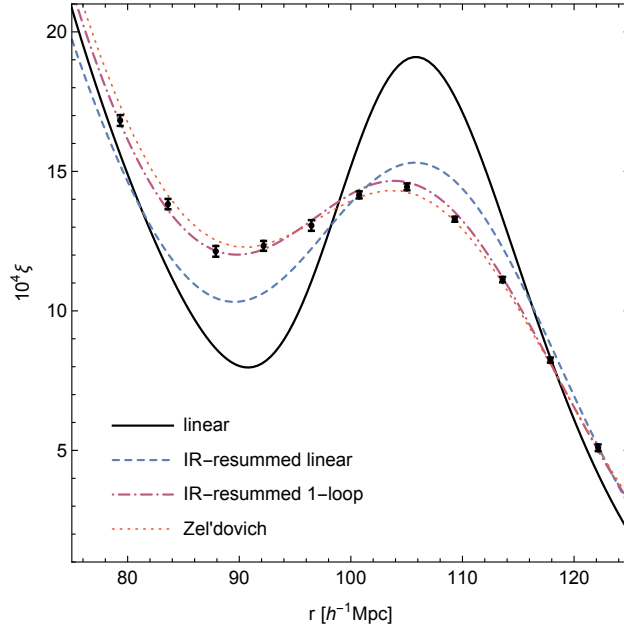
Figure 2: *Various theoretical approximations to the acoustic peak in the correlation function as well as simulati on measurements. Solid: linear, dashed: IR-resummed linear, dot-dashed: IR-resummed 1-loop, and dotted: Zel'dovich.*

using $\langle \exp(i\varphi) \rangle = \exp(-\langle \varphi^2 \rangle /2)$ if φ is a Gaussian variable, we obtain our final expression for the dressed two-point correlation function around $r \approx \ell_{\mathrm{BAO}}$

$$\tilde{\xi}_g(\boldsymbol{x}) \simeq \int \frac{\mathrm{d}^3\boldsymbol{k}}{(2\pi)^3} \, e^{i\boldsymbol{k}\cdot\boldsymbol{x}} e^{-\Sigma_{\epsilon k}^2 k^2} \, \langle \delta_g(\boldsymbol{k},t)\delta_g(-\boldsymbol{k},t)\rangle_\epsilon \,. \tag{87}$$

To write the exponent in the above form, we have used the fact that $\nabla^2 \approx \partial_r^2$ [and therefore $k^2 \approx (\hat{\boldsymbol{x}}\cdot\boldsymbol{k})^2$] up to corrections of order $\sigma/\ell_{\mathrm{BAO}}$. In principle, the exponential factor should only multiply the peak power $P_g^w(k)$, though in practice the smooth background at $r \approx \ell_{\mathrm{BAO}}$ is insensitive to the presence of this factor since $\Sigma \ll \ell_{\mathrm{BAO}}$. The subscript ϵ on the momentum space expectation value on the r.h.s. indicates that it should be evaluated in the absence of modes with momentum q smaller than ϵk, though it contains all short scale nonlinearities. Within a perturbative framework, it is possible to include dynamical effects of the long modes, as well as their non-Gaussianity by writing more complicated expressions.

The IR-resummed 1-loop EFT result in fig. 1 is obtained using this nonlinear treatment of modes with $q \ll k$. The resulting real-space correlation function is in very good agreement with the simulation results, as can be seen in fig. 2.

7 Lagrangian Perturbation Theory

Consider a fluid element that at time τ_0 is located at position $\boldsymbol{x}_0$. Its position at time τ is given by $\boldsymbol{x}_{fl}(\boldsymbol{x}_0, \tau_0; \tau)$ which satisfies:

$$\boldsymbol{x}_{fl}(\boldsymbol{x}, \tau; \tau') + \int_{\tau'}^{\tau} d\tau'' \boldsymbol{v}(\boldsymbol{x}_{fl}(\boldsymbol{x}, \tau; \tau''), \tau'') = \boldsymbol{x}. \tag{88}$$

It is convenient to define the (Lagrangian) location of a fluid element at the initial time $\boldsymbol{z}(\boldsymbol{x}, \tau) \equiv \boldsymbol{x}_{fl}(\boldsymbol{x}, \tau; 0)$. The displacement field is then defined as

$$\boldsymbol{\psi}(\boldsymbol{x}, \tau) = \boldsymbol{x} - \boldsymbol{z}(\boldsymbol{x}, \tau). \tag{89}$$

To make contact with the standard notation of the Lagrangian perturbation theory it is useful to invert the function $\boldsymbol{z}(\boldsymbol{x}, \tau)$ and express the displacement field in Lagrangian coordinates

$$\boldsymbol{\psi}(\boldsymbol{z}, \tau) = \boldsymbol{x}(\boldsymbol{z}, \tau) - \boldsymbol{z} = \int_0^{\tau} d\tau' \boldsymbol{v}(\boldsymbol{x}(\boldsymbol{z}, \tau'), \tau'). \tag{90}$$

From this definition it follows that

$$\dot{\boldsymbol{\psi}}(\boldsymbol{z}, \tau) \equiv \frac{\partial}{\partial \tau} \boldsymbol{\psi}(\boldsymbol{z}, \tau) = \boldsymbol{v}(\boldsymbol{x}(\boldsymbol{z}, \tau), \tau), \tag{91}$$

and

$$\ddot{\boldsymbol{\psi}} = D_\tau \boldsymbol{v} \equiv \left(\frac{\partial}{\partial \tau} + \boldsymbol{v} \cdot \nabla\right)\boldsymbol{v}, \tag{92}$$

where we introduced the convective derivative D_τ. Thus the Euler equation becomes:

$$\ddot{\psi}^i + \mathcal{H}\dot{\psi}^i + \frac{\partial}{\partial x^i}\phi = -\frac{1}{\bar{\rho}(1+\delta)}\frac{\partial}{\partial x^j}\tau^{ij}. \tag{93}$$

One can decompose ψ^i into a gradient and a curl piece and obtain equations for each of these pieces. For this purpose, one needs to express the Eulerian gradient of ϕ to Lagrangian derivatives of $\boldsymbol{\psi}$. From the mapping between Lagrangian and Eulerian space $\boldsymbol{x} = \boldsymbol{z} + \boldsymbol{\psi}$ and mass conservation

$$\bar{\rho} \, d^3\boldsymbol{z} = \bar{\rho}(1+\delta) \, d^3\boldsymbol{x}, \tag{94}$$

we have that $1 + \delta = 1/J$, where J is the determinant of the Jacobian matrix

$$A_{ij} \equiv \frac{\partial x_i}{\partial z^j} = \delta_{ij} + \partial_{z_j}\psi_i \tag{95}$$

where δ_{ij} is the Kronecker delta (not to be confused with density contrast). Spatial indices are raised and lowered using δ_{ij} and its inverse. Finally, we need to use

$$\frac{\partial}{\partial x_j} = A_{ij}^{-1} \frac{\partial}{\partial z_i}, \tag{96}$$

to express the derivatives with respect to x^i in terms of those with respect to z^i. Using these and the Poisson equation we can replace $\partial\phi/\partial x^i$ in terms of a nonlinear function of ψ^i and its derivatives. Solving this nonlinear eqution perturbatively is the goal of Lagrangian Perturbation Theory (LPT).

15. *Use* (89) *and* (94) *to obtain the following expression for δ in Fourier space*

$$\delta(\boldsymbol{k}) = \int d^3\boldsymbol{z} \ e^{i\boldsymbol{k}\cdot(\boldsymbol{z}+\boldsymbol{\psi})}. \tag{97}$$

7.1 Zel'dovich approximation

Suppose we ignore the stress tensor and linearize (93): To first order in ψ^i,

$$\delta^{(1)} = -\partial_i \psi^i, \tag{98}$$

and to the zeroth order, $A_{ij}^{(0)} = \delta_{ij}$, therefore

$$\frac{\partial}{\partial x^i}\phi = -\frac{3}{2}\Omega_m \mathcal{H}^2 \frac{\partial_i \partial_j}{\nabla^2}\psi^j + \mathcal{O}(\psi^2), \tag{99}$$

where spatial derivatives on the r.h.s. are all with respect to $\boldsymbol{z}$. We obtain (setting $\Omega_m = 1$)

$$\ddot{\psi}^i + \mathcal{H}\dot{\psi}^i - \frac{3}{2}\mathcal{H}^2 \frac{\partial_i \partial_j}{\nabla^2}\psi^j = 0. \tag{100}$$

As always, on an isotropic background the equations for the curl and gradient piece of $\boldsymbol{\psi}$ separate.

16. *Noticing that, by definition, $\boldsymbol{\psi}$ has to vanish at $\tau = 0$, show that the initial condition for $\boldsymbol{\psi}$ is curl-free.*

So we can solve for the divergence of ψ^i, which gives the same $\delta^{(1)}(\tau)$ obtained in section 3. Hence,

$$\boldsymbol{\psi}^{(1)}(\tau, \boldsymbol{k}) = -\frac{i\boldsymbol{k}}{k^2}a\delta_1(\boldsymbol{k}), \tag{101}$$

which is the displacement field we calculated in (76). Using (97), we obtain the first order Lagrangian solution for δ:

$$\delta_{\text{LPT}}^{(1)} = \int d^3\boldsymbol{z}\, e^{i\boldsymbol{k}\cdot(\boldsymbol{z}+\boldsymbol{\psi}^{(1)})}. \tag{102}$$

This is called the Zel'dovich approximation. Note that it contains terms of all orders in δ_1. However, if we want to know δ to order $\mathcal{O}(\delta_1^n)$, we have to calculate $\boldsymbol{\psi}^{(1)}, \boldsymbol{\psi}^{(2)}, \cdots, \boldsymbol{\psi}^{(n)}$ to be consistent. And one can show that the result would match what is obtained by using Eulerian perturbation theory. This must be the case since Lagrangian and Eulerian perturbation theories are solving the same equations but in terms of different variables.[5] However, the Zel'dovich approximation has two interesting properties:

Exactness in one-dimension: If we consider perturbations which only depend on one of the coordinates, say x^1, then we have an effectively $1d$ problem and the Zel'dovich approximation becomes exact before shell-crossing. This can be understood intuitively from the fact that in this approximation $\partial\phi/\partial x^i$ is calculated at linear order. Hence, the force on individual particles is set by the initial condition, without updating it as they move. However, in Newtonian gravity in $1d$ (or if we are talking about force of parallel infinite-sheets in $3d$) the force does not depend on the distance. It remains constant until particles cross one another (which is the definition of "shell-crossing"). Since the Eulerian equation (without τ^{ij}) is valid under the assumption that there is no shell-crossing, the Eulerian perturbation theory in this $1d$ set up is just the Taylor expansion of δ_{Zel} in δ_1.

On the other hand, shell-crossing happens eventually. And almost instantaneously, if we start from an initial power spectrum which has power at short scales. Thus the Zel'dovich approximation quickly fails to be exact, even in $1d$, and the same follows for the Eulerian perturbation theory. The counter-terms in τ^{ij} are needed to account for this failure.[6]

IR-resummation: The Zel'dovich approximation automatically resums the first order displacements. Hence, it gives a good prediction for the correlation function at BAO scale. See fig. 2.

---

[5] See 1511.01889 for a hybrid approach.

[6] This problem is studied in detail in 1502.07389 and 1710.01736.